






The Effect of Minimum Actuation Limit in Shape Control of a Single-Layer Dome Frame

Ahmed Manguri^{1,2,*} , Najmadeen Saeed^{2,3} , Farzin Kazemi¹ , Neda Asgarkhani¹ , and Robert Jankowski¹ 

¹Faculty of Civil and Environmental Engineering, Gdansk University of Technology, Gdansk, Poland

²Civil Engineering Department, University of Raparin, Iraq.

³Tishk International University, Erbil, Kurdistan Region, Iraq.

Article History

Received: 21.11.2022

Revised: 01.04.2023

Accepted: 18.02.2024

Published: 02.04.2024

Communicated by: Asst. Prof. Dr.

Abubakr M. Ashir

*Email address:

ahmed.manguri@pg.edu.pl

*Corresponding Author



Copyright: © 2023 by the author. Licensee Tishk International University, Erbil, Iraq. This article is an open access article distributed under the terms and conditions of the Creative Commons Attribution-NonCommercial 2.0 Generic License (CC BY-NC 2.0) <https://creativecommons.org/licenses/by-nc/2.0/>

Abstract:

This paper describes the significance of the minimum actuation limit per actuator while controlling the shape of a single-layer frame dome. The algorithms that perform optimum shape controlling allow the user to assign the minimum allowable actuation per actuator, which means the actuators with an actuation of less than the assigned amount are assumed to be passive; thus, they are excluded. In this study, the deformed shape of a numerical model of a single-layer dome is reshaped. At the same time, the minimum limit is assumed to vary between 0.1mm and 1 mm to investigate how the outcomes are affected. The results show that changes in the minimum allowable actuation significantly affect the number of necessary actuators and the final form of the structure in terms of nodal displacements and stresses. The study suggests using the limit of 0.7 mm, which provides the optimum number of actuators while the nodal displacements are controlled.

Keywords: *Dome Structures; Actuators; Actuation; Optimization; Structural Control*

1. Introduction

Dome structures are spatial structures built in tourist cities to attract visitors [1]. These architectural structures can be found in several countries, for example, in Kazakhstan [2], England [3], UAE [4], and Sweden [5]. Spatial structures may suffer noticeable deformation due to lateral loadings [6]. Since the appearance of such structures is significant, their imperfection should be eliminated or reduced by reforming them [7]. Researchers have been trying to improve the existing methods of shape control. Controlling nodal displacements was first introduced by Weeks in the early 1980s [8, 9].

The topic was further studied and developed by several researchers, and it was implemented on various structures. You [10] presented a technique to control the nodal displacements of a 2D plane cable net structure. Nyashin, Lkhov [11] described a method to nullify the joint displacements caused by external loadings. Furthermore, researchers applied techniques of shape controlling on different structures, such as cable-stayed bridges [12] and single-layer egg-shaped [13] structures. In general, the location of nodes can be controlled by changing the length of some active members, which can be done by actuators [14].

Generally, several actuators can be used to alter the length of members. Researchers have used different types of actuators for various purposes. Changing temperature by a specific value was used to change the length of spatial truss members' lengths [15]. Composite [16, 17] and flexible [18] structures were

embedded with piezoelectric actuators for shape control. Moreover, lead-active screw [19] and mechanical [12, 20] actuators were also implemented for shape control.

Structural optimization opened a new chapter in structural engineering, optimization algorithms used to minimize structural weight [21], topology optimization [22-24]. For the last three decades, researchers have been trying to minimize the number of actuators for bar length changing [25]. The location of turnbuckles can significantly affect their efficiency [26, 27]. Saeed, Manguri [28] presented a technique to find optimum actuator numbers to reshape cable structures. The optimum number of actuators was found for controlling pin-jointed assemblies [29] and minimizing the cross-sectional area of cables and trusses [30]. Actuator numbers were also optimized for double-layer hinged domes [31-33]. Other researchers like Chen, Jiang [34], Dhingra and Lee [35], and Du, Yue [36] studied actuators placement in optimal locations. However, reshaping structures using and optimizing the number of actuators has been studied, and researchers underestimated the minimum size of actuation per actuator.

This research details the effect of the minimum limit of actuation (MLA) on reshaping and optimizing the number of actuators. In this study, MATLAB software is used to determine the actuation. The found actuation is applied to the structure in MATLAB and SAP2000 to verify the results. The research plan is as follows: Section I describes the general introduction and literature review. It is followed by Section II, which presents the structure's numerical model of the research, then the results are discussed in Section III. Finally, the conclusions are summarized in Section IV.

2. Numerical Model

This section describes modeling the numerical structure, its physical propensities, and the loading case. The numerical model is 1.049 m high and 2 m wide; the height-to-width ratio is acceptable based on standards [37]. The radius of the numerical model was assumed to be 1000 mm. The coordinates of the joints were found based on the relationship between the nodes and the dome's radius, as presented in the MATLAB code lines 2-8 in Figure 1. An intensive MATLAB code to generate the models is presented in Figure 1. The dome is formed by 145 Nodes, as presented in Figure 2, and 384 Members (see Fig 3). Furthermore, Joints 1 to 25 are hinged in all directions. The members are made of 6mm in diameter aluminum, with a modulus of elasticity of 70000 MPa and a yield strength of 276 MPa.

The numerical model is horizontally loaded at joints 96 to 145 with 1280 N to get noticeable displacements. The horizontal load may represent any possible lateral load. In this research, the nodal displacements were controlled using the expression below.

$$(1) \quad -|d| - d_t \leq Y e_o \leq |d| - d_t$$

Where d is the induced nodal displacements due to external loadings, and $[-d_t \text{ to } d_t]$ is the domain of the joint displacements after adjustment.

```

Nr=24; Nc=6; %Nr:is number of base coordintes & Nc:is no. of circles
R=1000 ;Th=0;Alpha=0; j=0; % Raduis, horizontal and vertical angles
for i=1:Nc
    for i=1:Nr
        j=j+1; coor(j,1)= R*cosd(Alpha)*cosd(Th);
        coor(j,3)= R*cosd(Alpha)*sind(Th);
        coor(j,2)= R*sind(Alpha); Th=Th+360/Nr;
    end; Alpha=Alpha+90/Nc;end
coor=[coor;0 R/R/(Nc^2) 0;]%all nodal coordinates + top joint coordinate
nJ=size(coor,1);% Number of joints
for j=1:Nr*(Nc-1); % connecting the 24 nodes of each circle out of 6
    bar(j,1)=j+24; bar(j,2)=j+24+1; end
for i=1:Nc-1; % connecting the first and last node of ech circle
    Nare=Nr*i; bar(Nare,2)=(i)*Nr+1;end
for i=5*Nr+1:Nr*6 % connecting the top cicle nodes to the top node
    bar(i,1:2)=[i,145];end
for i=1:Nc-1 % Connecting the cicles to gether with V curved members
    for j=1:Nr
        bar((144+(i-1)*Nr+(j)),1:2)=[((i-1)*Nr+j) ((i-1)*Nr+j)+Nr ];end;end
for i=1:Nc-1 % Connecting the cicles together with V & H curved members
    for j=1:Nr
        bar((264+(i-1)*Nr+(j)),1:2)=[((i-1)*Nr+j) ((i-1)*Nr+j+Nr+1) ];end;end
for i=1:Nc-1; % connecting the first and last node of ech circle
    Nali=Nr*(i+1);bar(Nali,2)=i*Nr+1;end; Nami=size(bar,1);%barNumber

```

Figure 1: MATLAB code for generating the numerical model

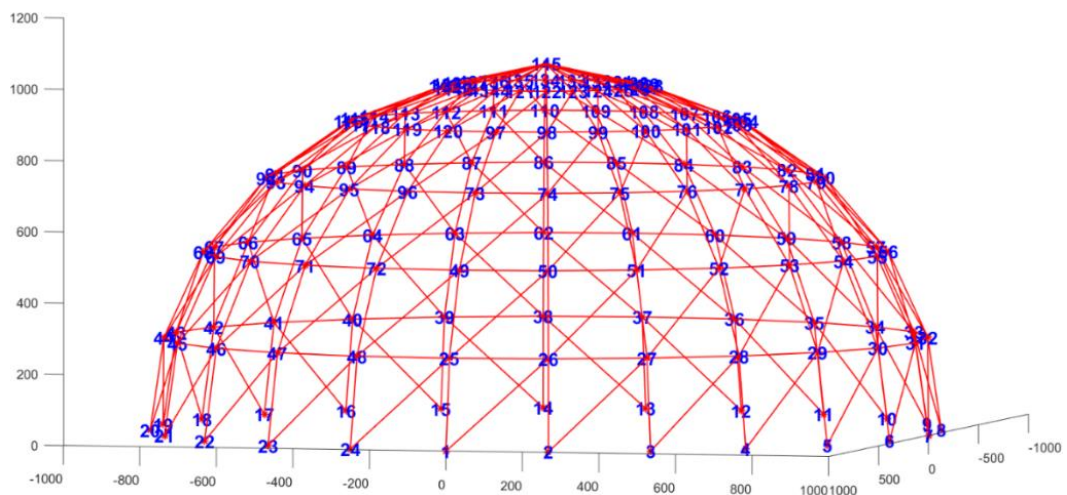


Figure 2: The joints of the numerical single-layer dome frame structure.

Y is a matrix assembled by linking the active members with the nodal displacements. Furthermore, (1) is subjected to the optimization function in (2) to find the most active members for controlling the nodal displacements. At the same time, the minimum and maximum limits of actuation are strictly considered via (3).

$$(2) \quad \min f(x) = \sum_{i=1}^n e_{oi}$$

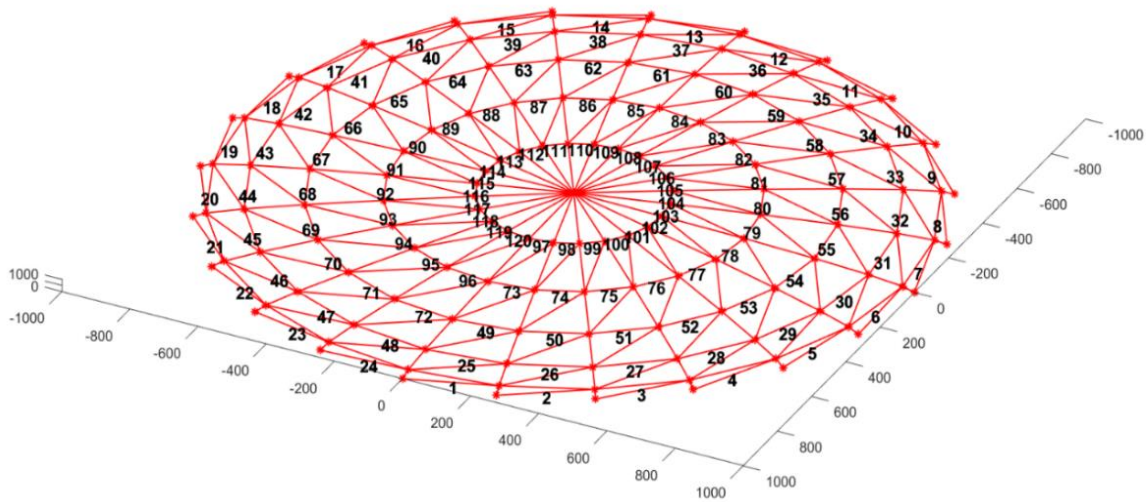


Figure 3: The members of the numerical single-layer dome structure.

Min $f(x)$ is a function defined as `fmincon` in MATLAB and relies on interior-point optimization algorithms. N is the number of actuators and e_o is the amount of actuation per actuator. The function searches for passive actuators in several iterations to exclude them from minimizing actuator numbers.

$$(3) \quad |L_b| \leq |e_o| \leq |U_b|$$

L_b and U_b are the domain of actuation per actuator; in this study, the domain is set to be ± 10 mm.

3. Results and Discussion

This study focuses on the effect of changing the minimum allowable actuation per actuator on the actuator numbers, nodal displacements, and internal forces after actuation. The absolute maximum induced nodal displacements in the X-direction ($\max(\text{abs}(dx))$), Y-direction ($\max(\text{abs}(dy))$), and Z-direction ($\max(\text{abs}(dz))$) are presented in Table 1. In addition, the maximum absolute internal forces, including axial force ($\max(\text{abs}(t))$), bending moment ($\max(\text{abs}(mom))$), and torsion ($\max(\text{abs}(tor))$), are presented in the table. The goal was to reduce the nodal displacements to ≤ 5 mm in all joints. The minimum actuation limit (MLA) was changed from 0.1 mm to 1 mm with 0.1 mm increments. Only three cases are shown, namely MLA= 0.1 mm, 0.5 mm, and 0.9 mm.

Table 1: Maximum absolute induced internal forces and maximum absolute induced displacements.

Max (abs (d_x))	Max (abs (d_y))	Max (abs (d_z))	Max (abs (t))	Max (abs (mom))	Max (abs (tor))
mm			N	N.mm	
14.68	9.91	2.65	7787	1676	1042

3.1 Case 1 (MLA=0.1 mm)

Figure 4 shows the minimization of actuator numbers and actuation amount for MLA=0.1 mm in 22 iterations. The actuator number in the last step is 84, while the actuation is 30. The figure also illustrates that the absolute maximum actuation increases in subsequent iterations. This is because the remaining ones take the effort of the excluded actuators.

The joint post-adjustment displacements for MLA=0.1 mm are presented in Fig 5. The results confirm that the nodal displacements after adjustment within the permitted domain except to iteration 2, dx_2 , are almost 5.3 mm. In addition, the changes of maximum absolute internal forces, including axial force

(t) moment (mom) and torsion (tor) in 22 iterations, are shown in Fig 6. An increase in the maximum axial forces and the bending moment can be observed from the 1st to the last iteration. In contrast, the maximum absolute torsion fluctuated in the middle iterations, but the value of the last iteration was almost the same as that of the first iteration.

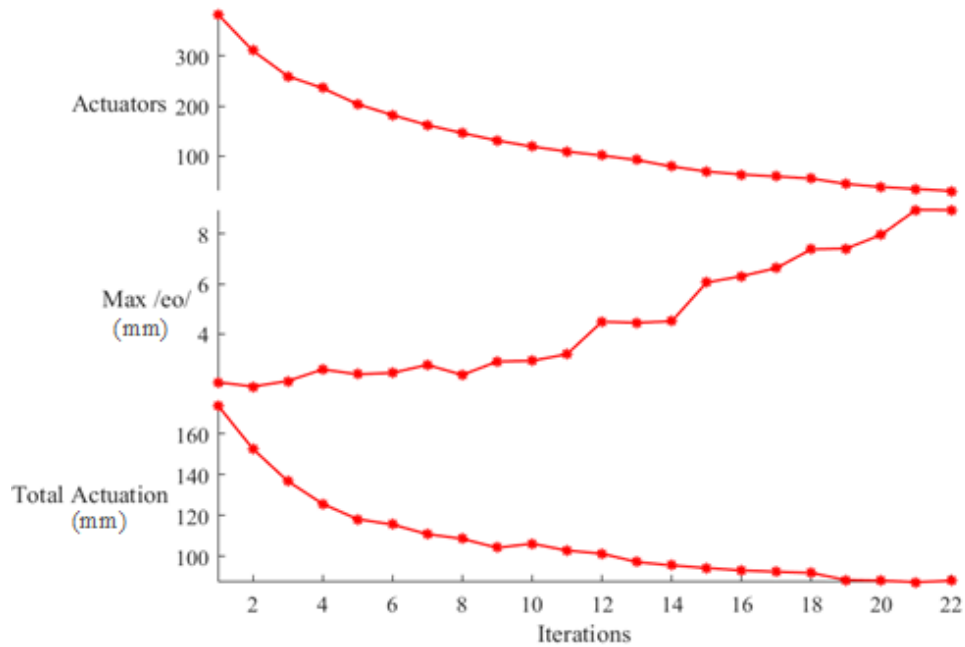


Figure 4: Actuator numbers and actuation in 22 iterations when MLA=0.1 mm.

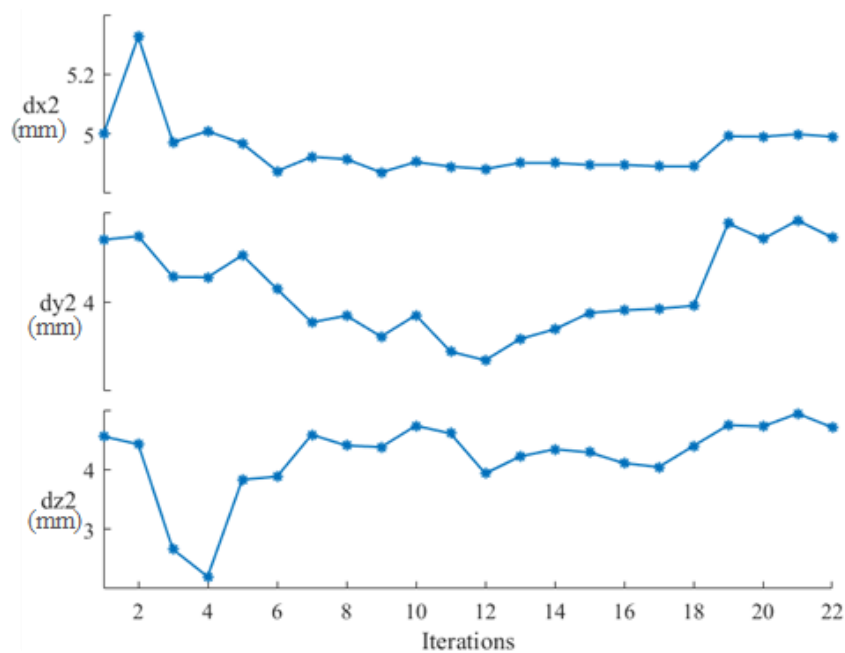


Figure 5: Maximum absolute displacements in 22 iterations when MLA=0.1 mm.

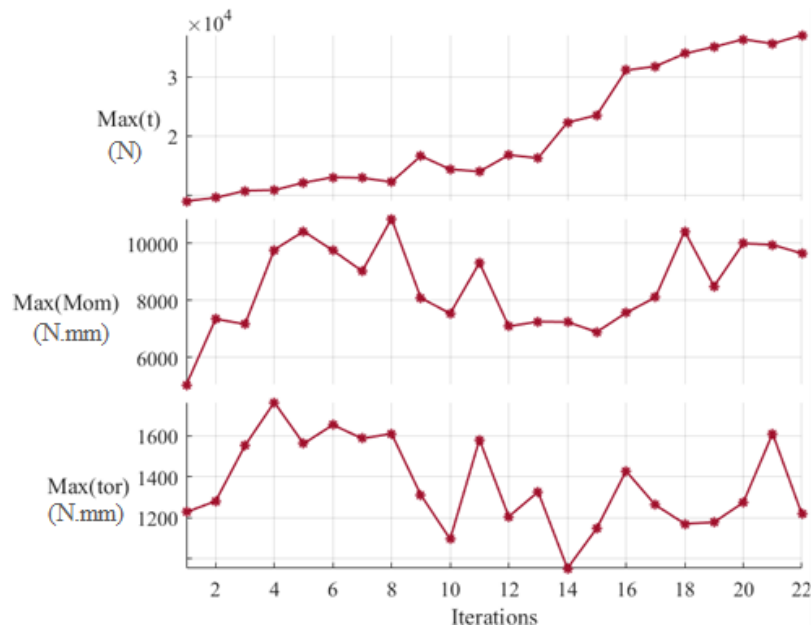


Figure 6: Maximum absolute internal forces in 22 iterations when MLA=0.1 mm.

3.2 Case 2 (MLA=0.5 mm)

In this case, the optimum solution was obtained in 7 iterations. Similar to case 1, the number of actuators and amount of actuation declined. In contrast, the absolute maximum actuation increased, as presented in Figure 7. The states of nodal displacements in 7 iterations are presented in Fig 8. The changes in the internal forces in 7 iterations are shown in Figure 9. Figure 8 confirms that the nodal displacements were controlled within the permitted limit. Moreover, Figure 9 shows an increase in the maximum absolute internal forces in subsequent iterations due to changing the length of the members by actuation.

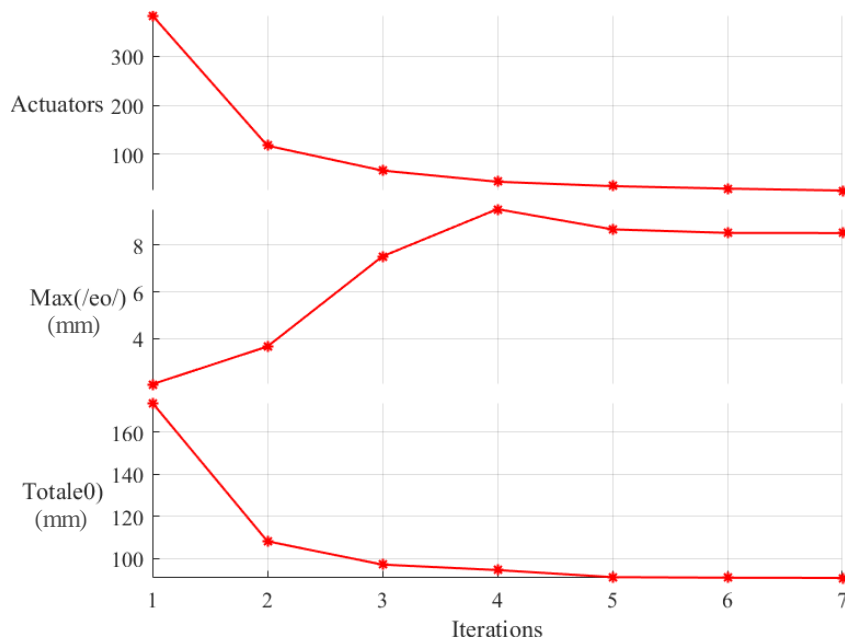


Figure 7: Actuator numbers and actuation in 7 iterations when MLA=0.5 mm.

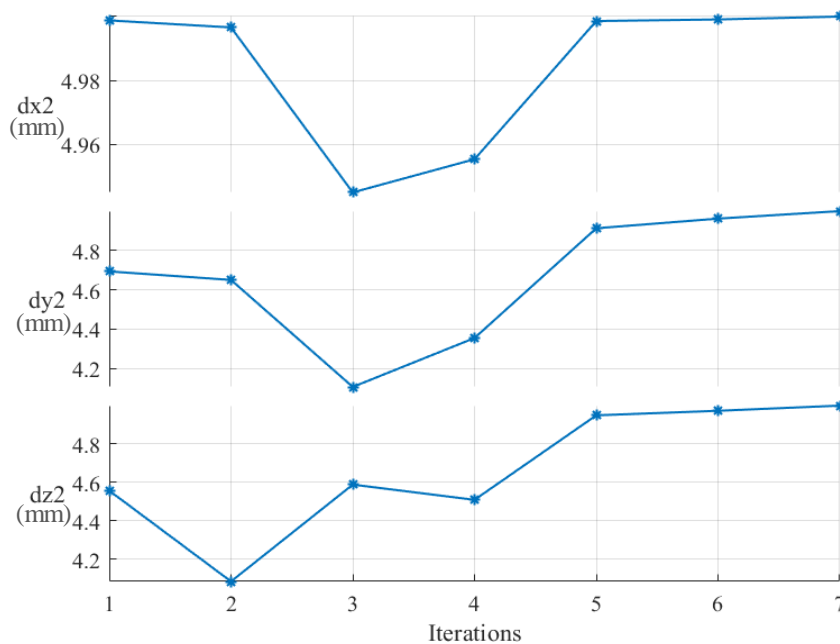


Figure 8: Maximum absolute displacements in 7 iterations when MLA=0.5 mm.

3.3 Case 3 (MLA=0.9 mm)

In this case, the optimum solution was obtained in 5 iterations, as presented in Figure 10. As in the previous cases, the actuator numbers and total amount of actuation dropped in subsequent iterations while the absolute maximum actuation increased. Figure 11 shows that the displacements exceeded the domains in iterations 4 and 5 since the actuation limit was increased and the number of actuators decreased. For this reason, iteration 3 should be taken as the optimum solution.

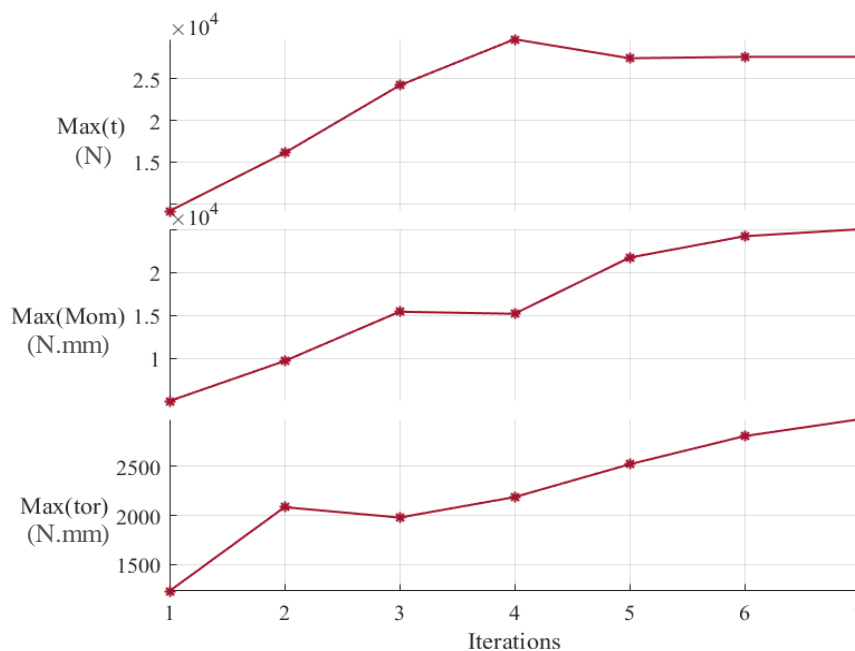


Figure 9: Maximum absolute internal forces in 7 iterations when MLA=0.5 mm.

3.4 The Optimal Case

Figure 12 shows that the optimum case can be when $MLA = 0.7$ mm, which provides the minimum number of actuators, which is 21. The optimum solution has been obtained in 6 iterations, which is less than the other MLAs except for $MLA = 0.9$ mm and 1, but the nodal displacements in these two cases passed the limit; thus, $MLA = 0.7$ mm gives the optimum solution. The figure shows that, when $MLA = 0.7$ mm, the maximum actuation is 10 mm, while the total actuation is just over 90 mm. Figure 13 illustrates the nodal displacements in the last iteration for all cases within the boundary except for the last two cases ($MLA = 0.9$ mm and $MLA = 1$ mm). Moreover, the internal forces in the last iterations fluctuated between $MLA = 0.1$ mm and $MLA = 1$ mm (see Figure 14). However, in this research, the internal forces were not controlled.

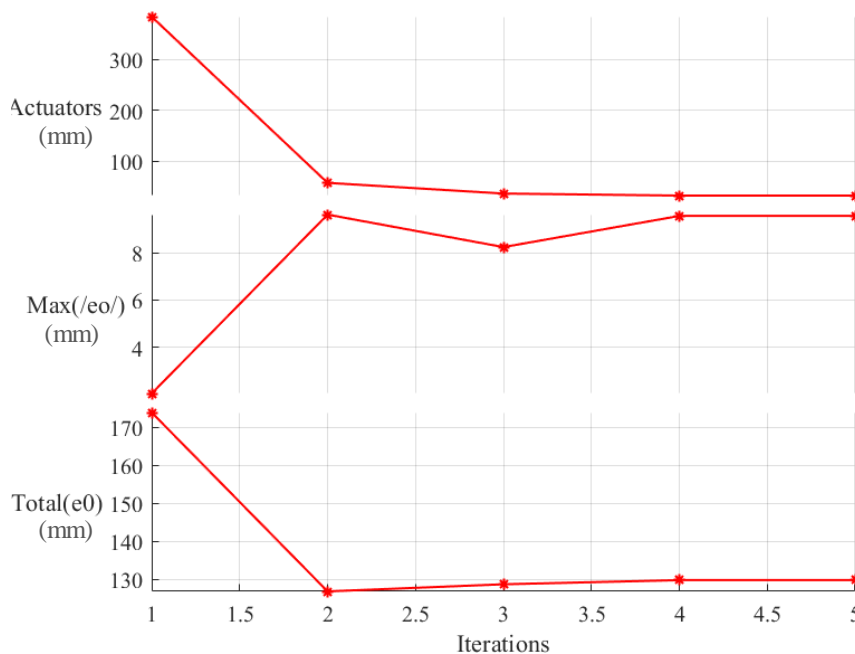


Figure 10: Actuator numbers and actuation in 5 iterations when $MLA = 0.9$ mm.

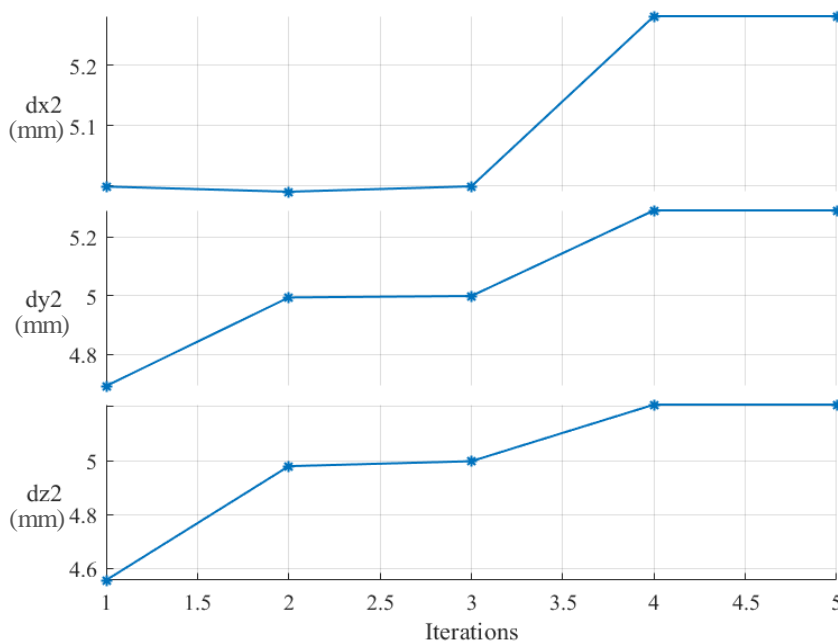


Figure 11: Actuator numbers and actuation in 5 iterations when $MLA = 0.9$ mm.

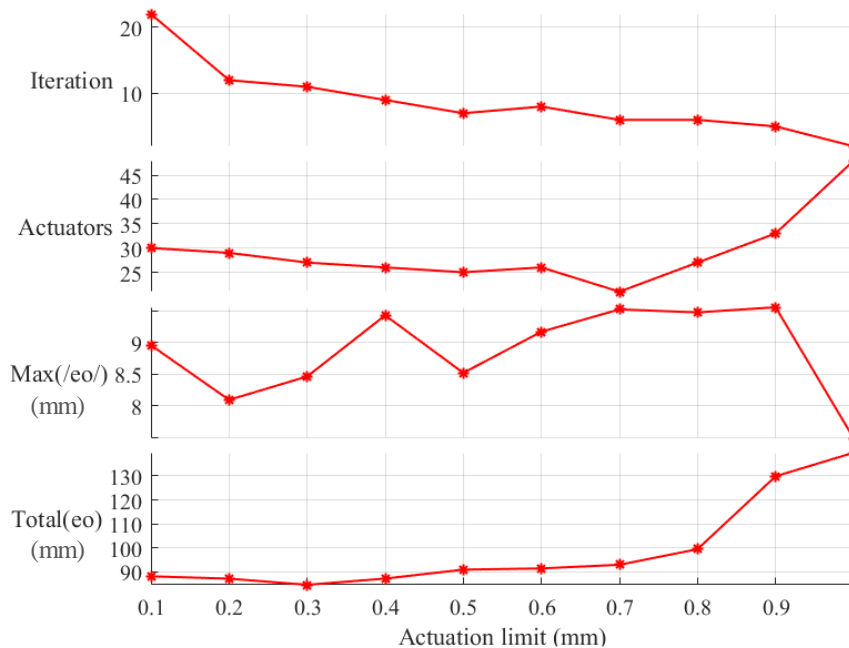


Figure 12: The number of iterations, actuator numbers, maximum absolute actuation, and total actuation for different MLA.

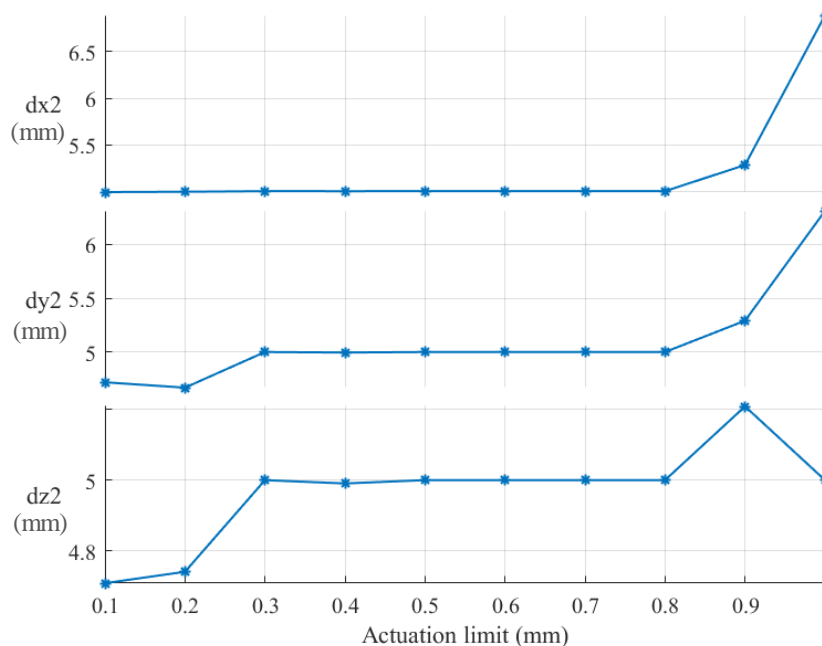


Figure 13: Maximum absolute displacements in the last iteration for 10 MLAs.

4. Conclusions

In this paper, different minimum limits of actuation (0.1 mm to 1mm with 0.1 increments) were tried to control the shape of a single-layer dome frame structure. The study aimed to find the best MLA that keeps displacement domains using minimum actuators. The nodal displacements were unleashed for each MLA to take any value in ± 5 mm in all directions. Meanwhile, members' axial force, bending moment and torsion were monitored. The effects of changing the MLA on minimizing iterations, actuators, and the total amount of action have been detailed. Moreover, the states of the internal forces, including axial force, bending moment, and torsion in members, were described for each MLA. The study found that the optimum MLA can be 0.7 mm, which involves minimum actuators (21 actuators) found in minimum iterations (6 iterations); meanwhile, the domain of the displacements was kept.

Furthermore, for the optimum case, the maximum actuation is 10 mm, and the total actuation is just over 90 mm.

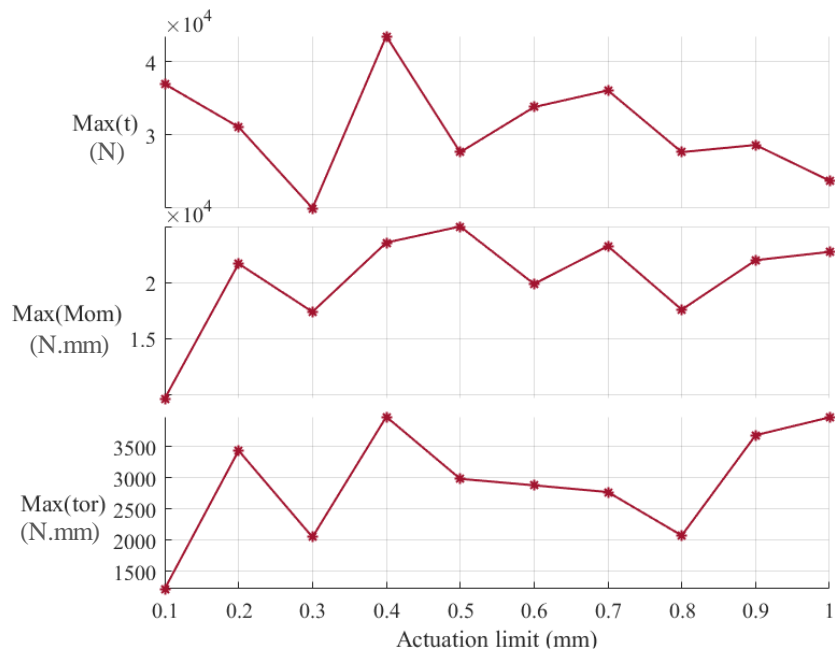


Figure 14: Maximum absolute internal forces in the last iteration for 10 MLAs.

6. Author's Contribution:

All authors conceived of the presented idea, M. A. and S. N. prepared the MATLAB code for generating the data., M. A. made data analysis, M.A., K. F., A. N., designed the graphs in MATLAB. M. A. wrote the first draft of the manuscript. All authors revised the manuscript. J. R. did the final revision of the manuscript.

"We confirm that all named authors have read and approved the manuscript. We also confirm that each author has the same contribution to the paper. We further confirm that all authors have approved the order of authors listed in the manuscript."

7. Conflict of Interest:

"There is no conflict of interest for this paper."

References

- [1] Bradshaw, R., et al., Special structures: past, present, and future. *Journal of structural engineering*, 2002. 128(6): p. 691-709. <https://doi.org/10.1061/ASCE0733-9445.2002.128:6691>.
- [2] Winterstetter, T., et al., Innovative Bautechnik im Herzen Asiens–die EXPO 2017 in Astana, Kasachstan. *ce/papers*, 2018. 2(1): p. 51-57. <https://doi.org/10.1002/cepa.630>.
- [3] Knebel, K., J. Sanchez-Alvarez, and S. Zimmermann, The structural making of the Eden Domes. *Space Structures*, 2002. 5(1): p. 245-254.
- [4] Imbert, F., et al., Concurrent geometric, structural and environmental design: Louvre Abu Dhabi, in *Advances in architectural geometry 2012*. 2013, Springer. p. 77-90.
- [5] Chang, X. and X. Haiyan. Using sphere parameters to detect construction quality of spherical buildings. in *2nd International Conference on Advanced Computer Control*. 2010 Shenyang, China: IEEE. <https://doi.org/10.1109/ICACC.2010.5487073>.

- [6] Mahmood, A., et al. Optimized Stress and Geometry Control of Spherical structures under Lateral Loadings. in *2022 8th International Engineering Conference on Sustainable Technology and Development (IEC)*. 2022. <https://doi.org/10.1109/IEC54822.2022.9807455>.
- [7] Manguri, A., N. Saeed, and B. Haydar. Optimal Shape Refurbishment of Distorted Dome Structure with Safeguarding of Member Stress. in *7th International Engineering Conference "Research & Innovation amid Global Pandemic"(IEC)*. 2021. Erbil, Iraq: IEEE. <https://doi.org/10.1109/IEC52205.2021.9476107>.
- [8] Weeks, C.J., Static shape determination and control of large space structures: I. The flexible beam. *Journal of Dynamic Systems, Measurement, and Control*, 1984. 106(4): p. 261-266. <http://dx.doi.org/10.1115/1.3140683>.
- [9] Weeks, C.J., Static shape determination and control of large space structures: II. A large space antenna. *Journal of Dynamic Systems, Measurement, and Control*, 1984. 106(4): p. 267-272. <https://doi.org/10.1115/1.3140684>.
- [10] You, Z., Displacement control of prestressed structures. *Computer Methods in Applied Mechanics and Engineering*, 1997. 144(1): p. 51-59. [http://dx.doi.org/10.1016/S0045-7825\(96\)01164-4](http://dx.doi.org/10.1016/S0045-7825(96)01164-4).
- [11] Nyashin, Y., V. Lokhov, and F. Ziegler, Stress-free displacement control of structures. *Acta Mechanica*, 2005. 175(1): p. 45-56. <https://doi.org/10.1007/s00707-004-0191-1>.
- [12] Manguri, A.A., A.S.K. Kwan, and N.M. Saeed, Adjustment for shape restoration and force control of cable arch stayed bridges. *International Journal of Computational Methods and Experimental Measurements*, 2017. 5(4): p. 514-521. <http://dx.doi.org/10.2495/CMEM-V5-N4-514-521>.
- [13] Saeed, N., et al. Shape Restoration of Deformed Egg-Shaped Single Layer Space Frames. in *2019 International Conference on Advanced Science and Engineering (ICOASE)*. 2019. Duhok, Kurdistan Region, Iraq: IEEE. <http://dx.doi.org/10.1109/ICOASE.2019.8723714>.
- [14] Irschik, H., A review on static and dynamic shape control of structures by piezoelectric actuation. *Engineering Structures*, 2002. 24(1): p. 5-11. [http://dx.doi.org/10.1016/S0141-0296\(01\)00081-5](http://dx.doi.org/10.1016/S0141-0296(01)00081-5).
- [15] Haftka, R.T. and H.M. Adelman, Effect of sensor and actuator errors on static shape control for large space structures. *AIAA Journal*, 1987. 25(1): p. 134-138. <https://doi.org/10.2514/3.9592>.
- [16] Koconis, D.B., L.P. Kollar, and G.S. Springer, Shape control of composite plates and shells with embedded actuators. I. Voltages specified. *Journal of Composite Materials*, 1994. 28(5): p. 415-458. <https://doi.org/10.1177/002199839402800503>.
- [17] Hadjigeorgiou, E., G. Stavroulakis, and C. Massalas, Shape control and damage identification of beams using piezoelectric actuation and genetic optimization. *International Journal of Engineering Science*, 2006. 44(7): p. 409-421. <https://doi.org/10.1016/j.ijengsci.2006.02.004>.
- [18] Hu, Y.-R. and G. Vukovich, Active robust shape control of flexible structures. *Mechatronics*, 2005. 15(7): p. 807-820. <https://doi.org/10.1016/j.mechatronics.2005.02.004>.
- [19] Salama, M., et al., Shape adjustment of precision truss structures: analytical and experimental validation. *Smart Materials and Structures*, 1993. 2(4): p. 240. <https://doi.org/10.1088/0964-1726/2/4/005>.
- [20] Manguri, A., N. Saeed, and R. Jankowski, Controlling nodal displacement of pantographic structures using matrix condensation and interior-point optimization: A numerical and experimental study. *Engineering Structures*, 2024. 304: p. 117603. <https://doi.org/10.1016/j.engstruct.2024.117603>.
- [21] Manguri, A., et al., Bending Moment Control and Weight Optimization in Space Structures by Adding Extra Members in the Optimal Locations. *Advances in Science and Technology Research Journal*, 2023. 17(4): p. 313-324. <https://doi.org/10.12913/22998624/169573>.
- [22] Li, X., et al., Topology optimization for prestressed cable-truss structure considering geometric nonlinearity. *Structural and Multidisciplinary Optimization*, 2023. 66(9): p. 201. <https://doi.org/10.1007/s00158-023-03646-1>.
- [23] Høghøj, L.C., et al., Simultaneous shape and topology optimization of wings. *Structural and Multidisciplinary Optimization*, 2023. 66(5): p. 116. <https://doi.org/10.1007/s00158-023-03569-x>.

- [24] Golecki, T., et al., Topology optimization of high-speed rail bridges considering passenger comfort. *Structural and Multidisciplinary Optimization*, 2023. 66(10): p. 215. <https://doi.org/10.1007/s00158-023-03666-x>.
- [25] Manguri, A., et al., Buckling and shape control of prestressable trusses using optimum number of actuators. *Scientific Reports*, 2023. 13(1): p. 3838. <http://dx.doi.org/10.1038/s41598-023-30274-y>.
- [26] Furuya, H. and R.T. Haftka, Placing actuators on space structures by genetic algorithms and effectiveness indices. *Structural Optimization*, 1995. 9(2): p. 69-75. <https://doi.org/10.1007/BF01758822>.
- [27] Kwan, A. and S. Pellegrino, Prestressing a space structure. *AIAA journal*, 1993. 31(10): p. 1961-1963. <https://doi.org/10.2514/3.11876>.
- [28] Saeed, N.M., A.A.H. Manguri, and A.M. Adabar, Shape and force control of cable structures with minimal actuators and actuation. *International Journal of Space Structures*, 2021. 36(3): p. 241-248. <https://doi.org/10.1177/09560599211045851>.
- [29] Saeed, N.M., et al., Static Shape and Stress Control of Trusses with Optimum Time, Actuators and Actuation. *International Journal of Civil Engineering*, 2023. 21(3): p. 379-390. <http://dx.doi.org/10.1007/s40999-022-00784-3>.
- [30] Manguri, A., et al., Optimum number of actuators to minimize the cross-sectional area of prestressable cable and truss structures. *Structures*, 2023. 47: p. 2501-2514. <https://doi.org/10.1016/j.istruc.2022.12.031>.
- [31] Saeed, N., A. Manguri, and S. Al-Zahawi. Optimum Geometry and Stress Control of Deformed Double Layer Dome for Gravity and Lateral Loads. in *2021 7th International Engineering Conference "Research & Innovation amid Global Pandemic"(IEC)*. 2021. Erbil, Iraq: IEEE. <https://doi.org/10.1109/IEC52205.2021.9476094>.
- [32] Manguri, A., et al., Optimal Reshaping and Stress Control of Double-Layer Spherical Structures Under Vertical Loadings. *Archives of Civil Engineering*, 2022. 68(4). DOI: <https://doi.org/10.24425/ace.2022.143056>.
- [33] Saeed, N., et al., Using Minimum Actuators to Control Shape and Stress of a Double Layer Spherical Model Under Gravity and Lateral Loadings. *Advances in Science and Technology Research Journal*, 2022. 16(6): p. 1-13. <https://doi.org/10.12913/22998624/155214>.
- [34] Chen, J., et al. Optimal Placement of Actuators for Active Vibration Control Using EER and Genetic Algorithm. in *2019 IEEE 10th International Conference on Mechanical and Aerospace Engineering (ICMAE)*. 2019. <https://doi.org/10.1109/ICMAE.2019.8880980>.
- [35] Dhingra, A.K. and B.H. Lee, Optimal placement of actuators in actively controlled structures. *Engineering Optimization*, 1994. 23(2): p. 99-118. <https://doi.org/10.1080/03052159408941347>.
- [36] Du, J., et al., Optimal Placement of Actuators Via Sparse Learning for Composite Fuselage Shape Control. *Journal of Manufacturing Science and Engineering*, 2019. 141(10). DOI: <https://doi.org/10.1115/1.4044249>.
- [37] Nie, G.-b., et al., Seismic performance evaluation of single-layer reticulated dome and its fragility analysis. *Journal of Constructional Steel Research*, 2014. 100: p. 176-182.